



Stopping anisotropy in molecular chains

S. Peter Apell^{a,b,*}, J. Aizpurua^{a,b}, John R. Sabin^c, S.B. Trickey^c

^a Department of Applied Physics, Chalmers University of Technology and Göteborg University, S-41296 Göteborg, Sweden

^b Donostia International Physics Center, San Sebastian, Spain

^c Quantum Theory Project, Department of Physics, University of Florida, Gainesville, FL 32611-8435, USA

Abstract

Recently, we have addressed the effects of overall shape upon the electronic response of isolated molecules and nanoclusters, with particular emphasis on the mean excitation energy. Here, we consider the relationship between gross molecular shape and mean excitation energy anisotropy for very long objects. In particular we compare results for elongated ellipsoids and a string of particles. We find the latter model gives a better prediction of stopping power anisotropies of isolated long molecules. © 2000 Elsevier Science B.V. All rights reserved.

1. Background

For most of the history of stopping calculations and measurements, the focus has been either bulk (crystalline) or very dilute gas (atomic) response. That history can be viewed as a focus upon the system (solid) and its isolated constituents (atoms). With increasing sophistication of both experimental and theoretical technique, as well as advances in material characterization and preparation, the evolution of charged particle energy deposition research would be expected to parallel the recent development of condensed matter physics: A broadening from study of bulk systems to include surfaces and nanoscale objects like quantum dots, Rydberg atoms, (finite) wires, and nanotubes. Clearly such assemblies have properties that can depend strongly on the relatively isolated nature of their constituents. In

many cases, those constituent entities are highly orientable. As chemists and material scientists become increasingly skillful at orienting long, more-or-less isolated molecular entities [1,2], it will be of growing importance to have interpretive predictions of orientation-related behavior.

This work addresses the characteristic anisotropy of stopping in *isolated*, very long molecules by connecting the extremes, namely, of stopping in simple, gas-phase atoms and in a single infinite chain of atoms, i.e., a thin wire. In other words we are delineating stopping behavior upon passing, in a global sense, from zero-dimensional to one-dimensional behavior. We devote particular attention to very asymmetric molecules (in the sense of long or high aspect ratio) since it is easy to anticipate that there will be more and more experimental results available for such molecules in well-controlled circumstances (e.g., aligned to avoid statistical averaging over directional properties). We find good correlation between our simple stopping model and results from detailed

* Corresponding author.

calculations on long molecules. The results may be expected to be relevant also for understanding the properties of, for example, metallic powders which tend to form strings of particles, chain-like dipolar systems [3] or brine-filled porous rock with similar geometrical patterns [4]. Another example of potential relevance comes from near-field optical microscopy. There has been recent interest in that area in rows of gold nanoparticles on an indium-tin-oxide doped glass [5]. Those rows are particularly relevant since the coupling between the particles was the basis for the observation of some unexpected features. Chains have also been suggested recently as having a strong absorption enhancement at long wavelengths because of structurally induced resonances [6].

Recently we have investigated the effects of molecular topology on the electronic structure and properties of molecules and nanoclusters [7] and their dependence on orientation with respect to the projectile beam. The main result was to establish a relationship between the mean excitation energy and the molecular ellipticity as defined from van der Waals radii. Good correlation was found with first-principles mean excitation energy calculations for a large class of molecules, thereby showing the importance of shape for an average quantity such as the mean excitation energy. That formalism is the point of departure for the present analysis.

For an axially symmetric target with its major axis aligned along the laboratory z axis, the linear energy deposition for a probe incident with laboratory frame velocity \mathbf{v} is [8]

$$-\left(\frac{dE}{di}\right) = nS^i(\mathbf{v}), \quad (1)$$

with i either $x = y$ or z and n the number density of scatterers. For a swift longitudinal beam (aligned along z), the stopping cross-section (SI units) is

$$S^z(v) = \frac{Z_1^2 Z_2 e^4}{4\pi m v^2 \epsilon_0^2} \ln \frac{2mv^2}{I_o^x}, \quad (2)$$

and for the transverse alignment

$$S^x(v) = \frac{Z_1^2 Z_2 e^4}{4\pi m v^2 \epsilon_0^2} \ln \frac{2mv^2}{\sqrt{I_o^x I_o^z}}. \quad (3)$$

Here Z_1, Z_2 are the projectile charge and the number of scattering electrons in the target molecule, respectively. In the Bethe approximation, the directional components I_o^i of the mean excitation energy are determined by the energy-dependent dipole oscillator strength distribution of the target, $f^i(E)$,

$$\ln I_o^i = \frac{\int f^i(E) \ln E dE}{\int f^i(E) dE}. \quad (4)$$

Evidently the directional difference in stopping cross-section for a single, fully axially symmetric system is

$$\Delta S(v) \equiv S^x(v) - S^z(v) = \frac{Z_1^2 Z_2 e^4}{8\pi m v^2 \epsilon_0^2} \ln \frac{I_o^x}{I_o^z}. \quad (5)$$

Clearly the ratio I_o^x/I_o^z is the parameter that characterizes the stopping anisotropy for such molecules. This ratio thus is the major object of our study. We will present results for two models of jellium systems.

2. Jellium ellipsoids

In this section we connect stopping and collective excitation energies via electron gas considerations. Such connections have a long history in stopping theory, dating to the homogeneous gas calculation of Kramers [9] and the related local plasma approximation of Lindhard and Scharff [10].

Finite, non-spherical jellium objects have proven to be a simple but powerful model for elucidating shape effect trends. Such objects have collective electronic dipolar excitation frequencies associated with the direction i which can be written as

$$\omega_p^i = \sqrt{n_i} \omega_p. \quad (6)$$

ω_p is the plasma frequency, hence is a measure of the density of the smeared-out ionic (jellium) background which by charge neutrality has to be the same as the electronic density. n_i is the so-called depolarization factor that is defined by geometry alone [11,12]. We do not consider the

bulk plasmon excitation since it is not shape-dependent and would drop out of Eq. (5). The simplest way to obtain Eq. (6) is to take the expression for the polarizability of a small (metal) particle (see e.g. [13]), introduce the free-electron-like Drude dielectric function and look for the poles of the polarizability which are the collective surface modes of the small particle.

The shape of a jellium ellipsoid of revolution with rotational axis c and semiaxes $a = b$ (i.e., a spheroid) satisfying

$$\frac{x^2}{a^2} + \frac{y^2}{b^2} + \frac{z^2}{c^2} = 1 \quad (7)$$

is determined uniquely by the eccentricity e

$$e = \frac{1}{c} \sqrt{|a^2 - c^2|}. \quad (8)$$

We assume the jellium ellipsoid to have sharp boundaries and to consist of a uniform electron gas. As we have shown within a heuristic scheme [7], because the plasma frequency is the only available energy scale, it follows that

$$\frac{I_o^x}{I_o^z} = \sqrt{\frac{n_x}{n_z}}, \quad (9)$$

independent of the actual value of ω_p . (At the risk of pointing out the obvious, this ratio applies to a single system. It is not a comparison of two different molecules.) This result can be confirmed on a more fundamental basis via the so-called Clemenger model [14] of cluster physics. Thus, the asymmetry ratio is expressed in terms of functions which only depend on shape. The depolarization factors ($0 \leq n_i \leq 1$) for a jellium ellipsoid can be written [13]

$$n_i = \frac{abc}{2} \int_0^\infty \frac{dp}{(j^2 + p)\sqrt{(a^2 + p)(b^2 + p)(c^2 + p)}}, \quad (10)$$

where $j = a, b, c$ in order when $i = x, y, z$. Consideration of a prolate ellipsoid leads, after some algebra, to a depolarization factor (in terms of eccentricity e) of

$$n_z = \frac{1 - e^2}{e^3} \left[\ln \sqrt{\frac{1+e}{1-e}} - e \right]. \quad (11)$$

For a spheroid where $a = b$,

$$n_x = n_y = \frac{1}{2}(1 - n_z) \quad (12)$$

since the n 's must sum to unity [13]. The ratio of the mean excitation energies perpendicular and parallel to the axis of rotation for such a jellium ellipsoid is then

$$\frac{I_o^x}{I_o^z} = \sqrt{\frac{1 - n_z}{2n_z}}. \quad (13)$$

Notice that this ratio is a function of a/c alone and is unity for $a = c$ (sphere). Thus the stopping anisotropy is solely a function of geometry in this model. It should be noted that the results above have no overall energy scale except ω_p , the plasma frequency.

The dashed curves in Fig. 1 show the dispersion of the two collective modes (Eqs. (6), (11) and (12)) as a function of the shape of the particle parameterized by a/c . (Also shown there are the results for a string of N pearls parameterized by $1/N$; see discussion below, e.g., Eq. (15).) Starting from the spherical shape ($a = c$), the separation of modes grows such that at the extreme of asymmetric shape ($a \ll c$) one mode goes completely soft and the other approaches a squared energy of $\frac{1}{2}\omega_p^2$. For

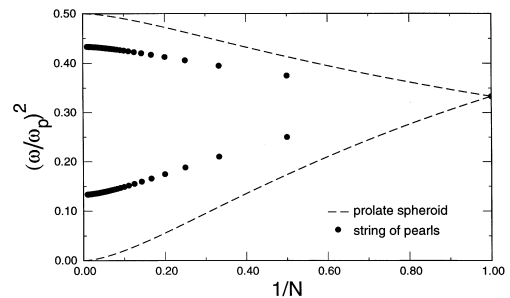


Fig. 1. Energies squared (in units of the plasma frequency squared) of the two collective modes of a jellium spheroid (dashed curves) as a function of its inverse aspect ratio a/c denoted as $1/N$ ($\alpha = 1$). Points give the corresponding modes for a chain of touching spheres ("string of pearls") as a function of the number N of spheres ("pearls") in the chain.

the purposes of the present analysis, this softening behavior is a drawback of the model, since the corresponding shapes prevent prediction of asymptotic features of very elongated molecules. (It should be pointed out in passing that a cylindrical model would have the same mode softening in the limit that the aspect ratio goes to infinity.) Hence we present a new approach in the next section.

Fig. 2 shows the mean excitation energy ratio from Eq. (9) as a function of inverse aspect ratio a/c ($a/c \rightarrow 0$ for very elongated objects, $a/c = 1$ for spherical ones). The divergence for small values of a/c is a direct manifestation of the mode softening shown in Fig. 1. Fig. 2 also provides a comparison with values for some representative molecules calculated via a much more sophisticated scheme [15]. In that calculation CH_4 corresponds to a *spherical* molecule in the present calculation and C_2H_2 is an example of a relatively high aspect-ratio molecule.

This simple model captures well the main physics involved. However, closer inspection of Fig. 2 shows that the longer molecule values are slightly below the theoretical prediction. It is also obvious as we go to longer molecules that the spheroidal model does not reproduce their shape accurately. Of necessity it introduces an incorrect curvature to the terminal electron distribution.

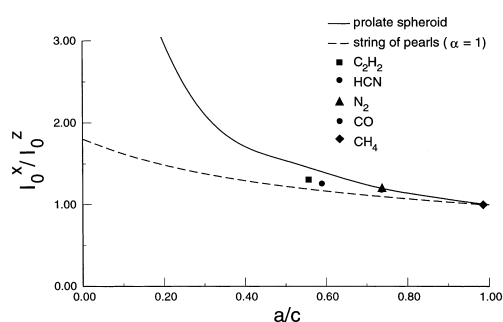


Fig. 2. Directional mean excitation energy ratio as a function of inverse aspect ratio c/a for a jellium spheroid (prolate $a \leq c$ only). The specific molecular anisotropies shown are from polarization propagator calculations [15]. The full curve comes from evaluating Eq. (9). The dashed line is our improved model, plotted as a function of the ratio between width and length of a chain of atoms. Note that in this case the mean excitation energy ratio does not diverge for small a/c (large N) because there is no mode softening in the case of the chain.

Therefore, the next section gives a description that permits consideration of extended objects without requiring the use of a spheroid as it becomes asymptotically long. This additional realism turns out to have beneficial effects on the ability to predict the directional mean excitation energy ratio and leads to a finite value for I_0^x/I_0^z when $a/c \rightarrow 0$.

3. A string of pearls

We introduce a model built from many spheres in a row, with the possibility of going from one to infinitely many. It is based on the so-called spectral representation of the response properties of a general chain of non-overlapping spheres with arbitrary separations (center-center distance σ) and sizes (sphere diameter d) [16]. Here, we consider only equidistant spheres of equal size but with variable filling fraction $\alpha = d/\sigma$. Hence α goes from zero for very separated spheres to unity for touching spheres. α is a purely geometrical quantity that, however, can be related to the interaction strength; see discussion after Eq. (16). As with the previous model, one can derive the depolarization factors and again they sum to unity, hence Eq. (12) holds but with [16]

$$n_z = \frac{1}{3}(1 - \alpha^3 F_N). \quad (14)$$

Now N is the number of spheres and F_N is a structure function discussed below. In terms of N and α we can relate the spheroidal inverse aspect ratio, a/c considered before, to the ratio between the width of the chain and its length as

$$\frac{a}{c} = \frac{d}{(N-1)\sigma + d} = \frac{\alpha}{\alpha + N - 1}, \quad (15)$$

which for touching spheres ($\alpha = 1$) assumes the simple form $a/c = 1/N$. Physically α is a measure of the filling fraction of the chain. Chemically α can be interpreted alternatively as a measure of the interaction or bonding strength between the constituent “atoms” (spheres) of the chain. Hence, the range of α spans the non-interacting to the fully interacting chain. Note that $\alpha \neq 1$ because the

model does not allow for overlapping spheres. Introduction of such overlap would add complexity well beyond the scope of the present study.

The function F_N , which contains the geometrical information is given by Fuchs [16] ($N > 1$)

$$F_N = \frac{1}{2N} \sum_{i=1}^N \sum_{j=i+1}^N \frac{1}{|j-i|^3}. \quad (16)$$

This we recognize as a so-called dipolar sum since it sums an interaction decaying as the third power of the inverse distance over all the “atoms” in the system. We retrieve specifically the one-dimensional dipolar sum for the infinite chain: $F_\infty = \frac{1}{2}\zeta(3) \approx 0.601$ (where ζ is the Riemann zeta function).

With definitions of F_N and a/c in hand for the string of pearls, we can use Eq. (14) in Eq. (6) to provide the dispersion of the two dipolar modes in the string-of-pearls model as a function of the geometrical factor α and the number of atoms in the chain N . It is convenient to do this first for $\alpha = 1$ as a function of $1/N$. This case is shown as points in Fig. 1. It is clear that the modes for the string of pearls are qualitatively different for the very long, high aspect-ratio objects. In particular there is no mode softening. This difference obviously has important consequences for the mean excitation energy ratio and in fact remedies that specific shortcoming of the spheroidal model in the limit of very long objects.

The ratio of mean excitation energies for the chain is

$$\frac{I_o^x}{I_o^z} = \sqrt{\frac{n_x}{n_z}} = \sqrt{\frac{1 + \frac{1}{2}\alpha^3 F_N}{1 - \alpha^3 F_N}}. \quad (17)$$

Since $F_\infty < 1$ and $\alpha \leq 1$, the ratio in Eq. (17) is finite in the limit of very long molecules as opposed to the infinite value in the spheroidal model. To relate Eq. (17) to geometrical parameters for long molecules we must find reasonable measures of bonding distances and radii of the constituent atoms. Here, we do not pursue those issues but refer to our previous papers where a thorough discussion is given [7]. Instead we use $\alpha = 1$ since this is the best case to illustrate the qualitative differences

between the two models of stopping asymmetry we consider.

Fig. 2 shows the mean excitation energy ratio from Eq. (17) as a function of $a/c = 1/N$ ($\alpha = 1$), as determined via Eq. (15). It is readily apparent that the chain has less variation for long molecules, mainly because there is no mode softening in this model (see comparison of dispersion for the two models in Fig. 1). The string-of-pearls model also gives a better account of the first-principles numerical calculations [15] than does the prolate spheroidal curve. Our main emphasis has been to introduce a qualitative change to indicate how the problem with the divergence in the spheroidal model can be avoided. In a geometrical sense, we have used a model which approximates the molecular shape from the opposite perspective from that of the spheroidal model. Clearly the true results are in between the two curves. Also notice that we have used one α -value to represent the different molecules in order to indicate the main features of the string-of-pearls model. In reality there would be a different α -value for each molecule. The determination of $\alpha(a/c)$ for real molecules might seem somewhat arbitrary. However, the values of a/c in the figure assigned to the actual molecules were determined from the canonical van der Waals radii of their constituents. Additional details of this procedure are given in [7]. In any case, these models are semi-quantitative at most, hence, no purpose would be served by trying

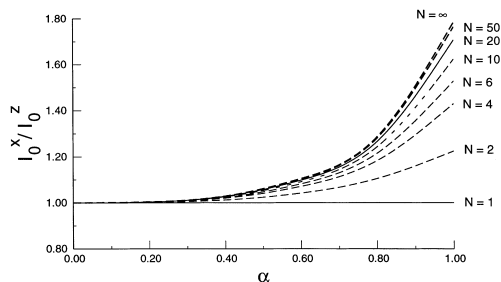


Fig. 3. Illustration of the way the directional mean excitation energy ratio changes in passing from one atom ($N = 1$) to infinitely many as a function of the filling fraction α ($\alpha = 1$ corresponds to touching spheres), i.e., how this ratio changes with dimensionality going from zero-dimensional to one-dimensional.

to tune the model parameters to yield quantitatively reliable results.

To appreciate the α -dependence, i.e., the importance of the filling fraction or degree of interaction in the chain, which is both of physical and chemical interest, Fig. 3 shows the directional mean excitation energy ratio as a function of α for a chain with one up to an infinite number of atoms. Again $\alpha = 1$ is the touching situation and $\alpha = 0$ is the extreme dilute limit corresponding to one sphere. As such, Fig. 3 accounts for the possible spread in directional mean excitation energies on the far left in Fig. 2. Fig. 3 also illustrates the relationship between directionality in stopping and the dimensionality of a system.

4. Conclusions

An amusing consequence of Eq. (17) is that an infinite string of vanishingly small ($d \rightarrow 0$) objects with non-vanishing spacing (σ finite) is nearly *isotropic* in its stopping. A moment's reflection shows that this is not as odd a result as it might seem at first thought: The stopping of an arbitrarily small electronic distribution with finite electron density must tend to zero, hence the anisotropy of even an infinitely long chain of such objects must tend to zero also.

The string-of-pearls model provides semi-quantitative predictive power regarding longer molecules which is useful both for understanding trends and for calibrating what to expect before embarking on demanding first-principles calculation of such large systems. As with the spheroidal jellium model however, limitations will emerge if we want to address more detailed questions than the ones in this paper. In those cases one must go a step farther in refinement and use a treatment such as the boundary charge method [17]. It is a simplified numerical scheme useful for doing stopping and energy loss calculations on more complicated

geometries which are not easily amenable to the kind of models we have presented in this paper.

Acknowledgements

This work was supported in part by grants from the Swedish Natural Science Research Council and Iberdrola S.A. Chemistry Department of University of Southern Denmark, where some of this work was completed, is acknowledged for its warm hospitality.

References

- [1] J. Michl, E.W. Thulstrup, *Spectroscopy with Polarized Light*, Verlag Chemie, Weinheim, 1986.
- [2] B. Friedrich, D. Herschbach, *J. Phys. Chem.* 95 (1991) 8118.
- [3] C. Wijers, *J. Phys. C* 10 (1983) 397.
- [4] F. Claro, F. Brouers, in: M. Cardona, J. Giraldo (Eds.), *Proceedings of the Fifth Latin American Symposium on Surface Physics, Thin Films and Small Particles*, World Scientific, Singapore, 1989, p. 166.
- [5] J.R. Krenn, A. Dereux, J.C. Weeber, E. Bourillot, Y. Lacroute, J.P. Goudonnet, G. Schider, W. Gotschy, A. Leitner, F.R. Aussenegg, C. Girard, *Phys. Rev. Lett.* 82 (1999) 2590.
- [6] A.V. Vagov, A. Radchik, G.B. Smith, *Phys. Rev. Lett.* 73 (1994) 1035.
- [7] S.P. Apell, S.B. Trickey, J.R. Sabin, *Phys. Rev. A* 58 (1998) 4616.
- [8] H.H. Mikkelsen, J. Oddershede, J.R. Sabin, E. Bonderup, *Nucl. Instr. and Meth. B* 100 (1995) 451.
- [9] H.A. Kramers, *Physica* 8 (1947) 401.
- [10] J. Lindhard, M. Scharff, *Kgl. Dan. Vidensk. Selsk.: Mat.-Fys. Medd.* 27 (1953) 15.
- [11] J.A. Osborn, *Phys. Rev.* 67 (1945) 351.
- [12] E.C. Stoner, *Philos. Mag.* 36 (1945) 803.
- [13] L.D. Landau, E.M. Lifshitz, *Electrodynamics of Continuous Media*, Pergamon Press, Oxford, 1960.
- [14] K. Clemenger, *Phys. Rev. B* 32 (1985) 1359.
- [15] S.P.A. Sauer, J.R. Sabin, J. Oddershede, *Nucl. Instr. and Meth. B* 100 (1995) 458.
- [16] R. Fuchs, F. Claro, *Phys. Rev. B* 39 (1989) 3875.
- [17] J. Aizpurua, A. Rivacoba, N. Zabala, F.J. García de Abajo, *Surf. Sci.* 402–404 (1998) 418.